

# Double side interconnection for vertical power components based on macro and nano structured copper interfaces and printed circuit board technologies

7<sup>th</sup> Micro/Nano-Electronics Packaging and Assembly, Design and Manufacturing Forum  
May 22-23 2019 – WTC GRENOBLE France

Bojan DJURIC<sup>12</sup>, Vincent BLEY<sup>2</sup>, Julien MORAND<sup>1</sup>, Olivier DAGUT<sup>2</sup>,  
Jean-Pascal CAMBRONNE<sup>2</sup>, Stefan MOLLOV<sup>1</sup>

<sup>1</sup>Mitsubishi Electric  
R&D Centre Europe  
1, allée de Beaulieu CS 10806  
35 708 RENNES CEDEX 7  
France

<sup>2</sup>Université de Toulouse;  
UPS; INPT; LAPLACE;  
118 rte de Narbonne – Bât. 3R3  
CNRS; LAPLACE;  
F-31062 Toulouse France

Introduction

Context

Manufacturing process

Experimental results

Conclusion

Stronger power ratings ensured by



1. Interleaved topologies : Multicellular structures

- Reducing of passive components size
- Active components multiplying

2. Switches improvement : Wide band gap materials

- Increasing of switching frequency
- Higher working temperature

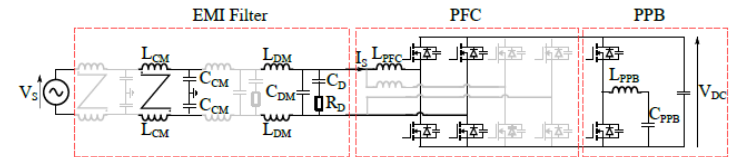


Figure 1: 3.3 kW ac/dc converter with SiC power devices

Active switches integration is sought



1. Reduce stray elements (and size)
2. Enhancement of thermal management (reliability)

## Motivation

### Electrical challenges

#### 1. Parasitic inductances

Overtoltage due to high  $di/dt$  ( $L_{PC}$  &  $L_{PE}$ )  
Slow down switching time ( $L_{PG}$  &  $L_{PE}$ )

#### 2. Parasitic capacitances

Ringing with parasitic inductances ( $C_{PCE}$ )  
Common mode current ( $C_{P OUT}$ )

#### 3. Parasitic resistances

Voltage drop

### Heat dissipation from

#### 1. Switches losses

#### 2. Interconnections losses (especially wire-bonds)

### Reliability

#### 1. Different CTE combined with thermal cycling

#### 2. Capable of handling many thermal cycling before failure

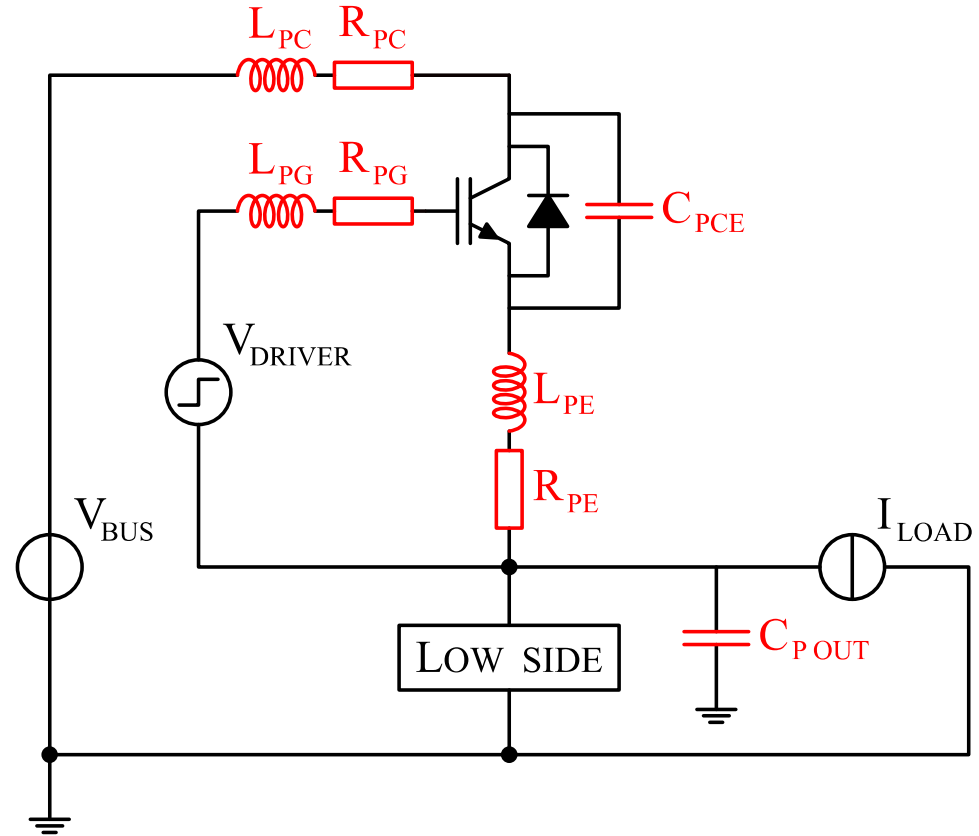


Figure 2: Zoom on parasitic elements (red) of the high side switching cell induced by the packaging

Introduction

Context

Manufacturing process

Experimental results

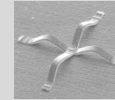
Conclusion

## Interconnection state-of-the-art

### Bonding

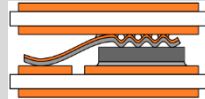


Wire bonding

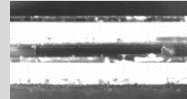


Ribbon bonding

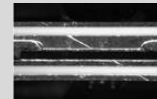
### Soldering



Bimetallic ribbon



Direct solder



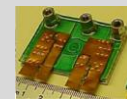
Metal post



Solder bump

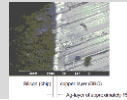


Direct lead bonding

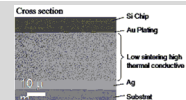


Dimple array

### Sintering

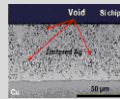


Low Temperature Joining Technology



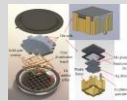
Low Temperature and Pressureless Sintering Tech.

### Diffusion bonding

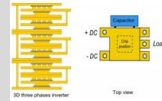


Transient Liquid Phase Bonding

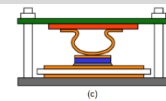
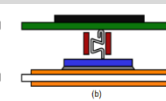
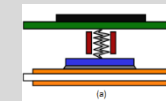
### Pressed



Press pack

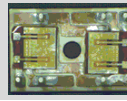


Low force 3D



Springs

### Electroplating



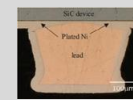
Power Overlay



Embedded Power

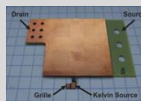


SiPLIT

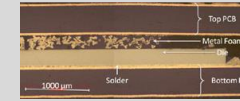


Nickel Micro Plating Bonding

### PCB technologies

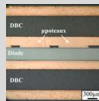


Micro vias

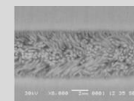


Foams

### Structured interface



Micrometric scale (post)



Nanometric scale (tube and wire)

## Printed Circuit Board (PCB)

### Printed Circuit Board (PCB) technology is

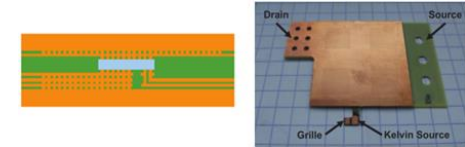
- Cost efficient and well-established process
- Offering massive parallel manufacturing
- Capable of fine pitch and able to use thick copper (heat and current transport)
- Accurate repeatable multilayer structures
- Fan-out capable
- Minimizing of loop size (stray inductances)

### PCB-embedding offers

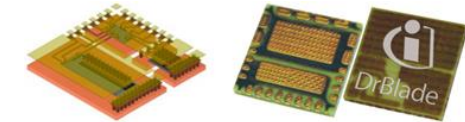
1. Double sided thermal dissipation and shorter heat path
2. Short interconnections and low parasitics
3. Increasing power density (by size reducing)

### Laser micro vias

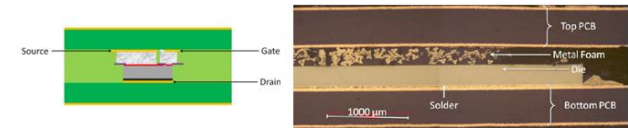
- Is the trend in PCB embedding interconnection
- Suffer of heat flux limitations (manufacturing limits)



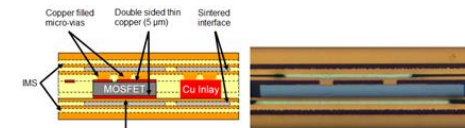
*Full  $\mu$ Vias interconnections*



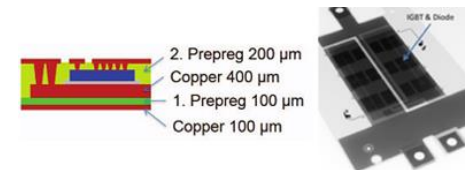
*diffusion bonding and  $\mu$ Vias interconnections*



*Soldering and foam interconnections*



*Galvanic Cu and vias interconnections*



*$\mu$ Vias and sintering interconnections*

## Assembly

### Proposed solution combines

- PCB substrates **(a)**
- having a macro post and nano wires interconnection
- sandwiching a die **(d)** surrounded of core **(c)**
- assembled by thermo-compression of prepregs **(b)**

### High level of integration

1. Double-side cooling possible (symmetrical structure)
2. Full copper and flexible interconnection
3. Expected resistant to cyclical stresses
4. Elementary block for power converter

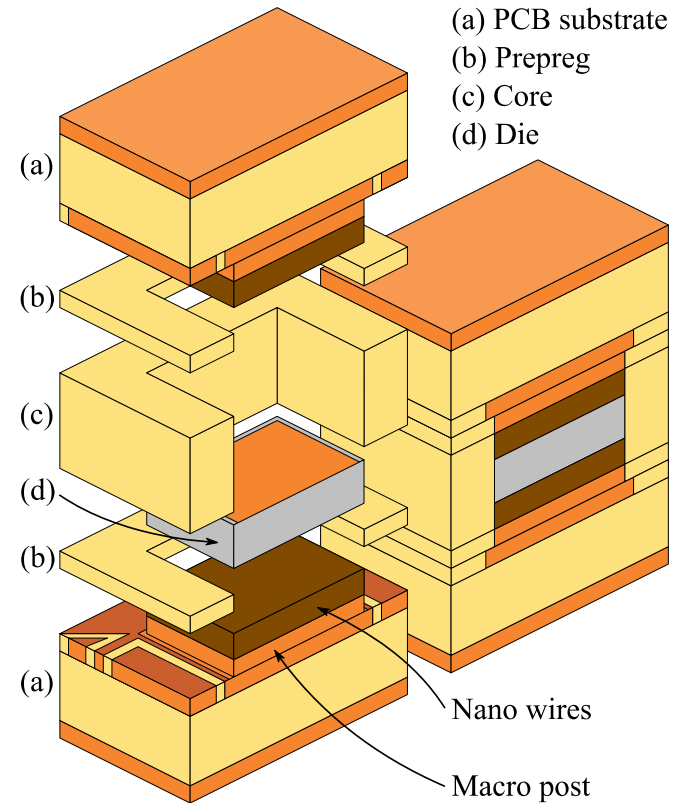


**Figure 3: Cross section schematic of the assembly with macro and nano structured interfaces**

Introduction

Context

Manufacturing process

Experimental results

Conclusion

## PCB substrate functions

A 0.8 mm high temperature core with two 105  $\mu\text{m}$  thick copper layers

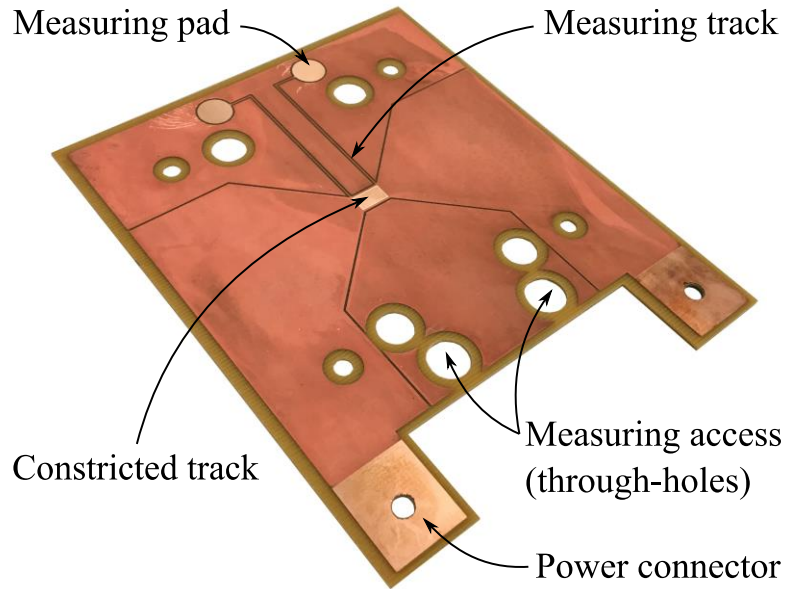


**Figure 4: PCB substrate with constricted area, its connectors and kelvin measuring tracks**

### Power connectors

- For electrical and thermal characterization

### Constricted area

- Bare copper area for the interconnection manufacturing
- Constriction is done for helping thermal characterization

### Measuring pads and tracks

- Additional contacts for Kelvin measurements

### Measuring accesses

- To the opposite substrate measuring pads

Brown oxidized remainder copper and ground planes to increase prepreg adhesion

## Interconnection

- **Opened dry film on constricted area**
  - a. Dry film deposition ( $\approx 45 \mu\text{m}$ ) on the whole PCB surface;
  - b. Opening of the dry film over the constricted area.

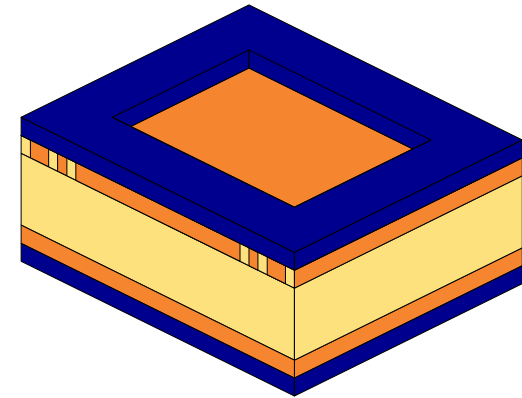


**Figure 5: Manufacturing process of interconnection on the PCB substrate**

## Interconnection

Opened dry film on constricted area

➤ **Copper electro-etching on the constriction**

- a.  $\approx 7 \mu\text{m}$  copper electro-etching (pulsed waveform) to increase adhesion of the surface.

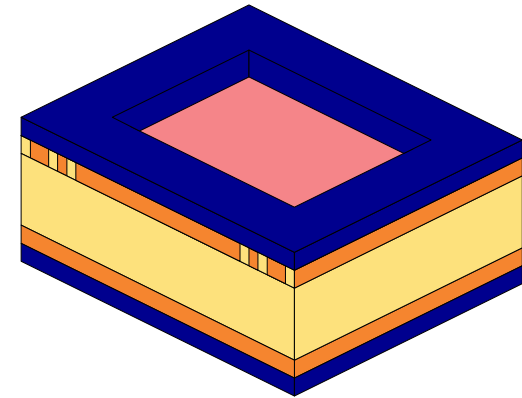


Figure 5: Manufacturing process of interconnection on the PCB substrate

## Interconnection

Opened dry film on constricted area  
Copper electro-etching on the constriction

➤ **Macro post electroplating (overflowing of dry film)**

- a.  $\approx 60 \mu\text{m}$  copper electroplating (pulsed waveform)  
The electroplating profile is adjusted to have the top of the post slightly higher than the dry film to ensure a complete filling of the cavity.

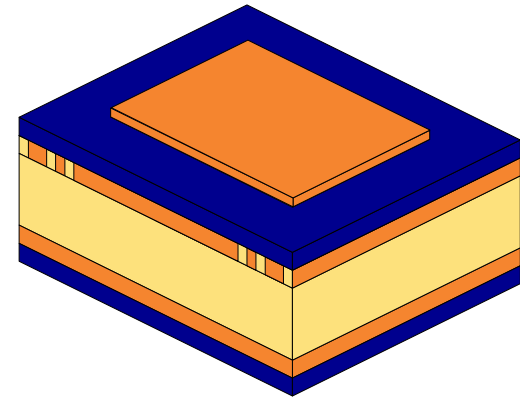


Figure 5: Manufacturing process of interconnection on the PCB substrate

## Interconnection

Opened dry film on constricted area  
Copper electro-etching on the constriction  
Macro post electroplating (overflowing of dry film)

### ➤ Leveling of the macro post by electro-etching

- a.  $\approx 7 \mu\text{m}$  copper electro-etching (pulsed waveform)  
The copper post is etched to obtain a flushed surface between the dry film and the copper post. This is the condition to ensure a correct sealing for the forthcoming steps.

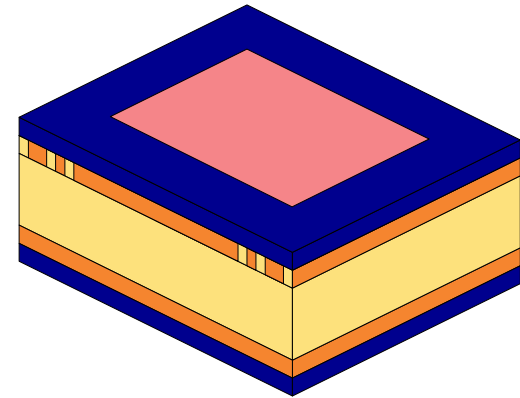


Figure 5: Manufacturing process of interconnection on the PCB substrate

## Interconnection

Opened dry film on constricted area  
Copper electro-etching on the constriction  
Macro post electroplating (overflowing of dry film)  
Leveling of the macro post by electro-etching

### ➤ Nano wires electroplating by pressed anode

- A nanoporous membrane is placed on top of the copper post;
- A solution of copper sulfate is spread over to act as an initiator;
- 2 layers of cellulosic papers are added on top as solution buffer;
- A copper anode is pressed on top of this assembly;
- Copper is electroplated during  $\approx 1$  hour through the membrane using a pulsed waveform.

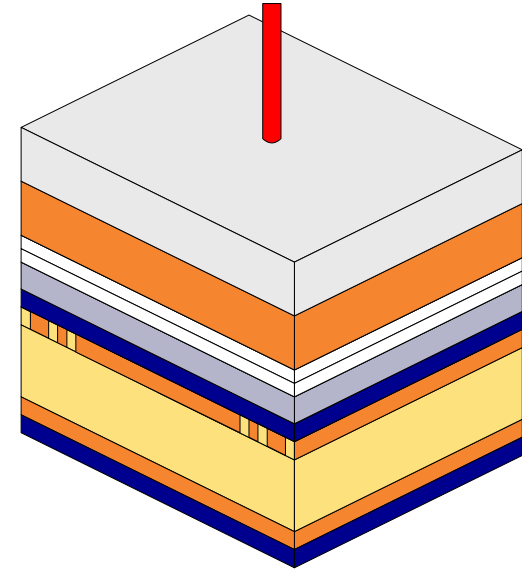


Figure 5: Manufacturing process of interconnection on the PCB substrate

## Interconnection

Opened dry film on constricted area  
Copper electro-etching on the constriction  
Macro post electroplating (overflowing of dry film)  
Leveling of the macro post by electro-etching  
Nano wires electroplating by pressed anode

### ➤ **Membrane filling by distanced anode**

Once the electrodeposition have been initiated

- The 2 layers of cellulosic papers are removed;
- The anode is placed further away;
- ≈ 6 hours copper electroplating is done until the membrane is filled.

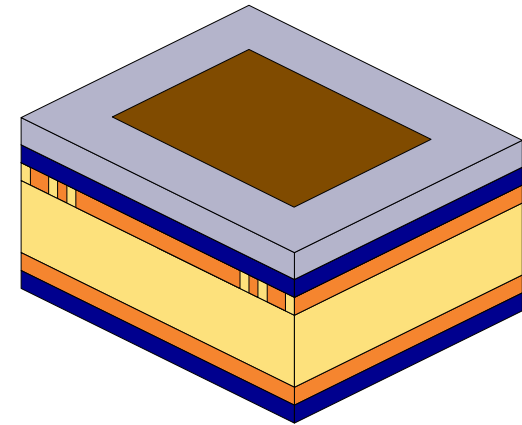


**Figure 5: Manufacturing process of interconnection on the PCB substrate**

## Interconnection

Opened dry film on constricted area  
Copper electro-etching on the constriction  
Macro post electroplating (overflowing of dry film)  
Leveling of the macro post by electro-etching  
Nano wires electroplating by pressed anode  
Membrane filling by distanced anode

### ➤ Dry film and membrane removal

- a. Sodium hydroxide treatment at 45°C during half an hour.

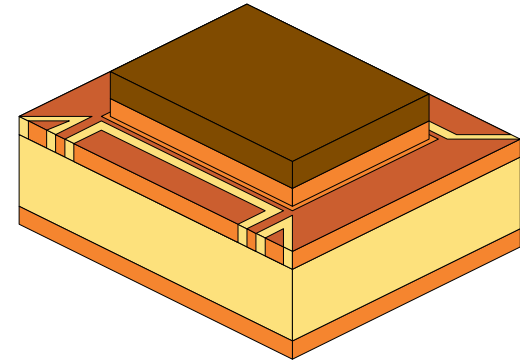


**Figure 5: Manufacturing process of interconnection on the PCB substrate**

## Interconnection

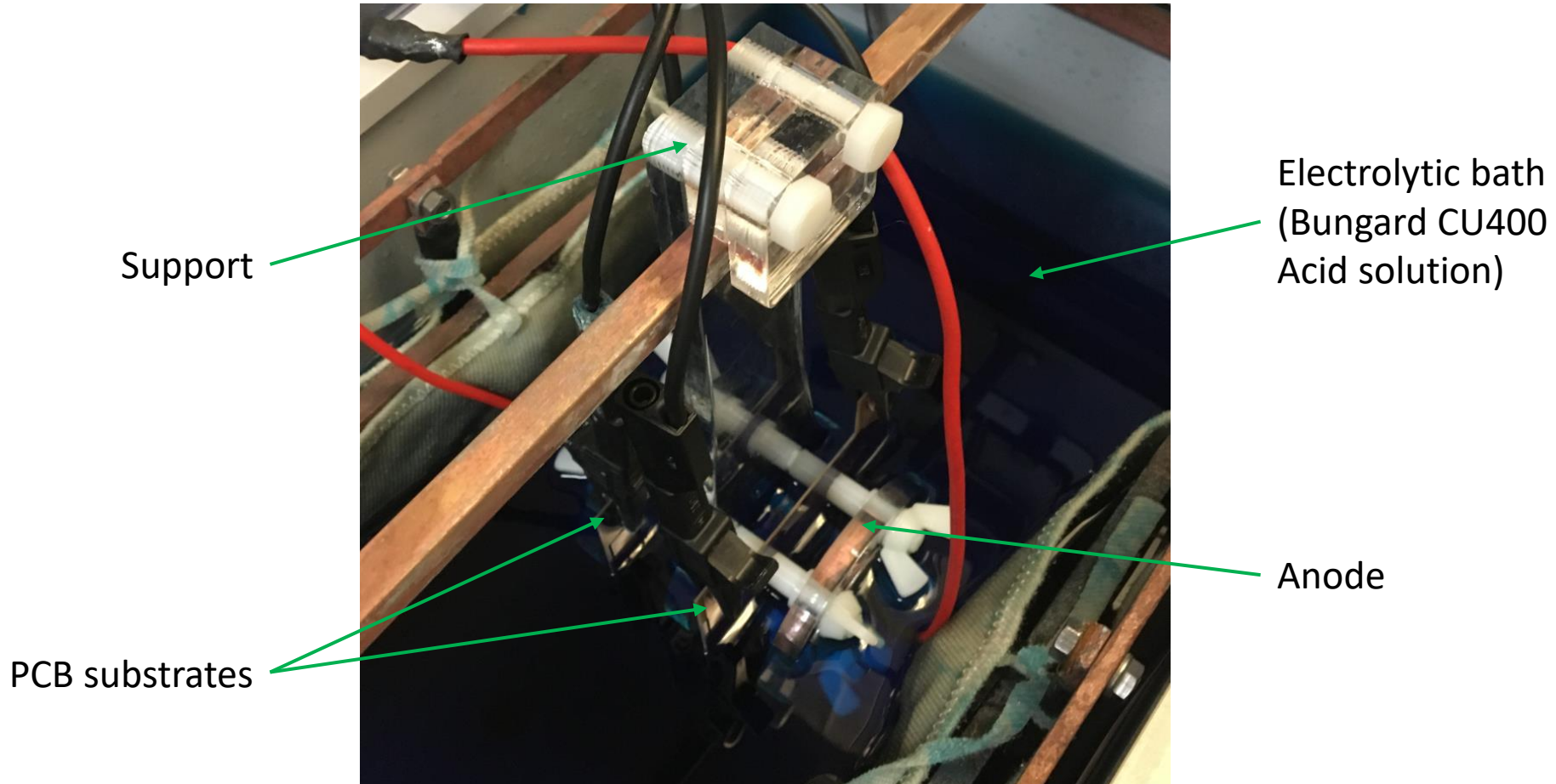


**Figure 6: Nano wires electroplating on 2 parallel substrates with Bungard COMPACT A equipment**

## Interconnection

Full copper interconnection : 45  $\mu\text{m}$  macro post and 55  $\mu\text{m}$  nano wires of 200 nm diameter

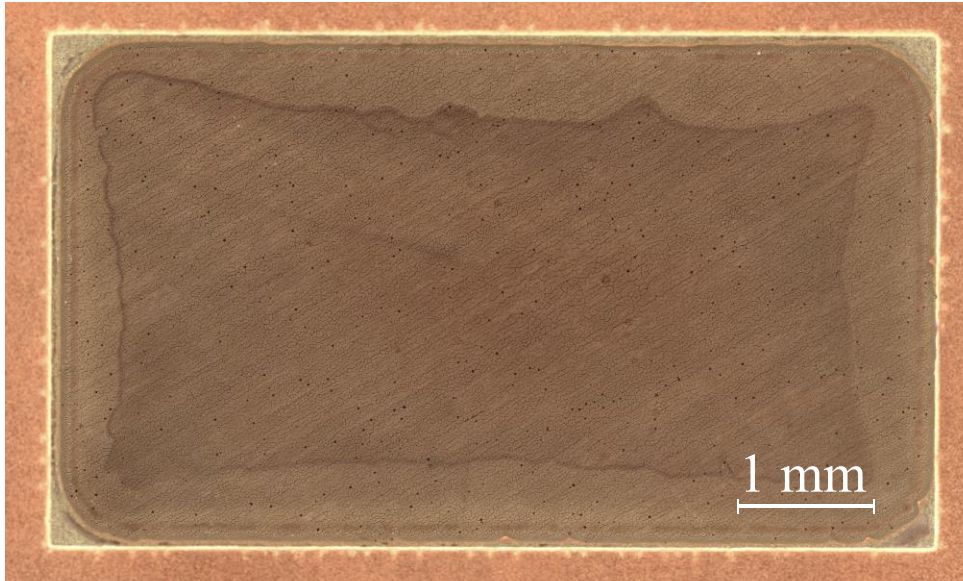


Figure 7: Digital microscope picture (x200) of the macro and nano structured interface

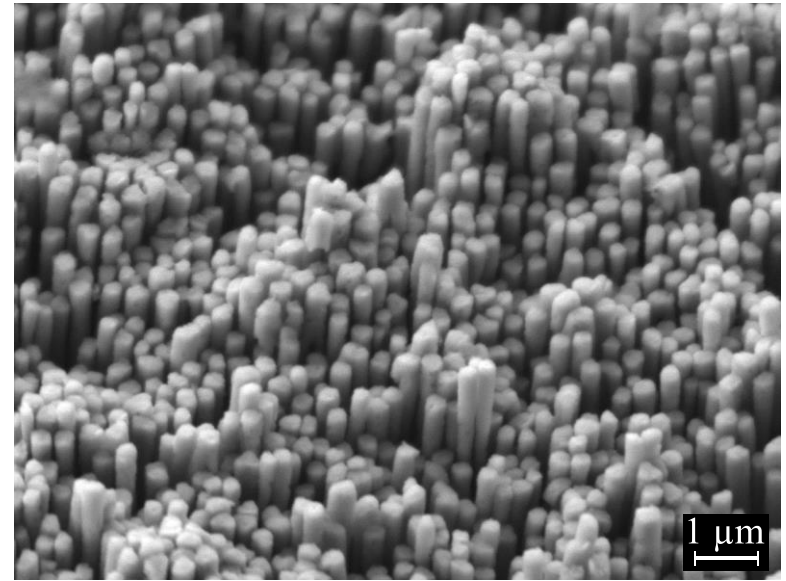


Figure 8: SEM acquisition (x10,000) of the nano wires 40° tilted top view

- Consistent and continuous = good heat and current transport
- Nano wires well separated = flexible stress resistant interface

## Test vehicles assembly

### ➤ Preparation of the support

- a. Bottom plate;
- b. 4 centering pins;
- c. 1st release film;
- d. Conformable press pad;
- e. 2nd release film.

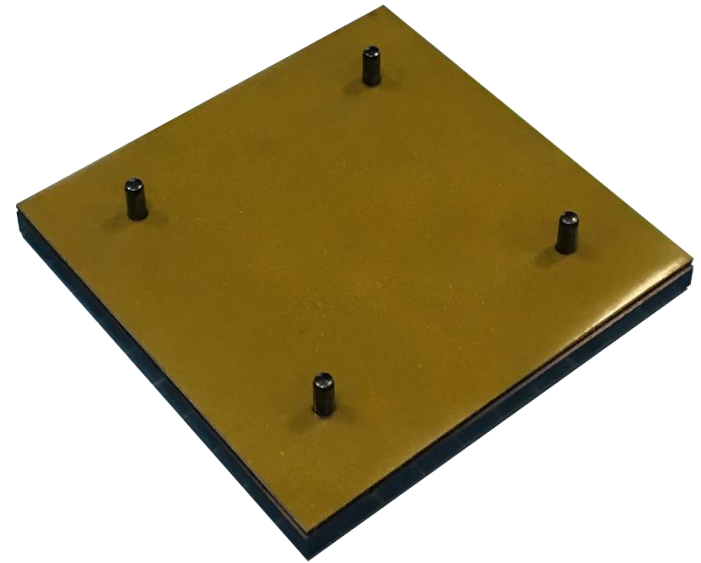


Figure 9: Stacking of the different elements of the prototype

## Test vehicles assembly

### Preparation of the support

#### ➤ Macro-nano structured PCB substrate

- a. Deoxidized by 10% sulfuric acid treatment;
- b. 12 hours annealing at 120°C.

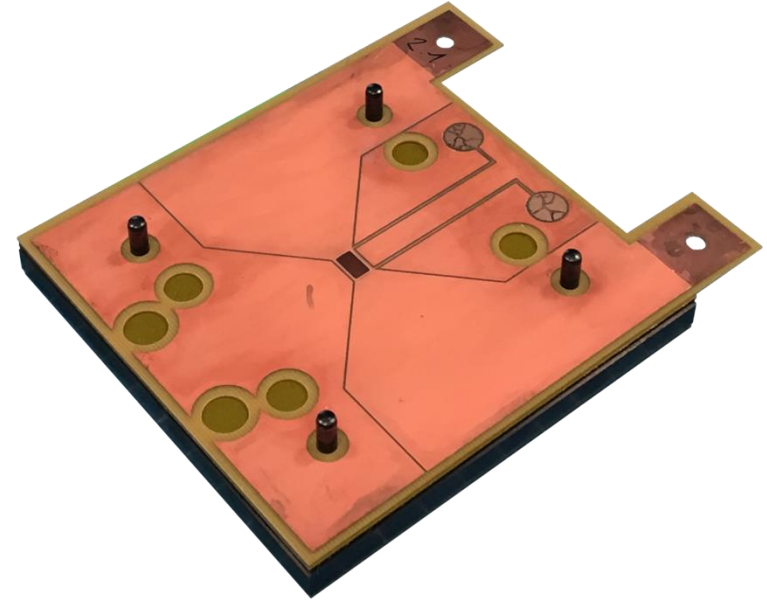


Figure 9: Stacking of the different elements of the prototype

## Test vehicles assembly

Preparation of the support  
Macro-nano structured PCB substrate

➤ **Prepreg Arlon 35N 106**

a. Laser cut-out.

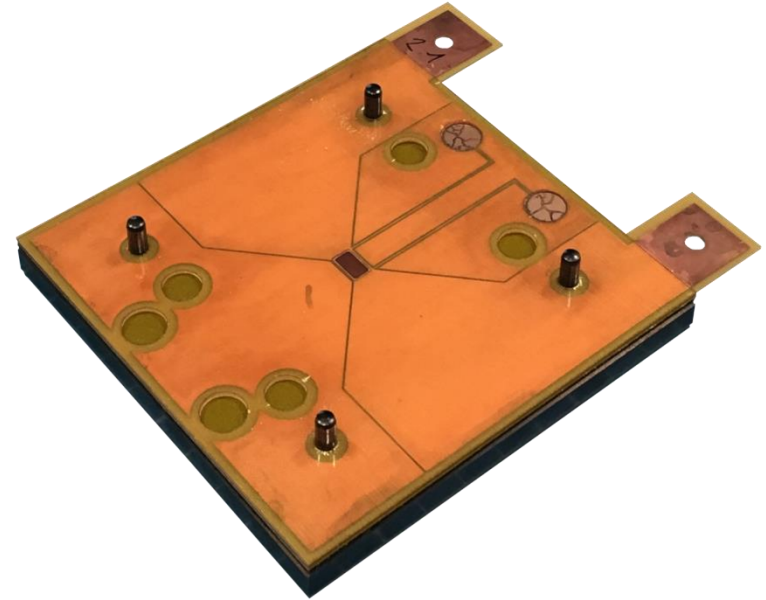


Figure 9: Stacking of the different elements of the prototype

## Test vehicles assembly

Preparation of the support

Macro-nano structured PCB substrate

Prepreg Arlon 35N 106

### ➤ Core Arlon 35N

- a. Stratification of prepregs Arlon 35N  
(1 × 2116, 1 × 1080 and 2 × 106);
- b. Through holes and routing by CNC device.

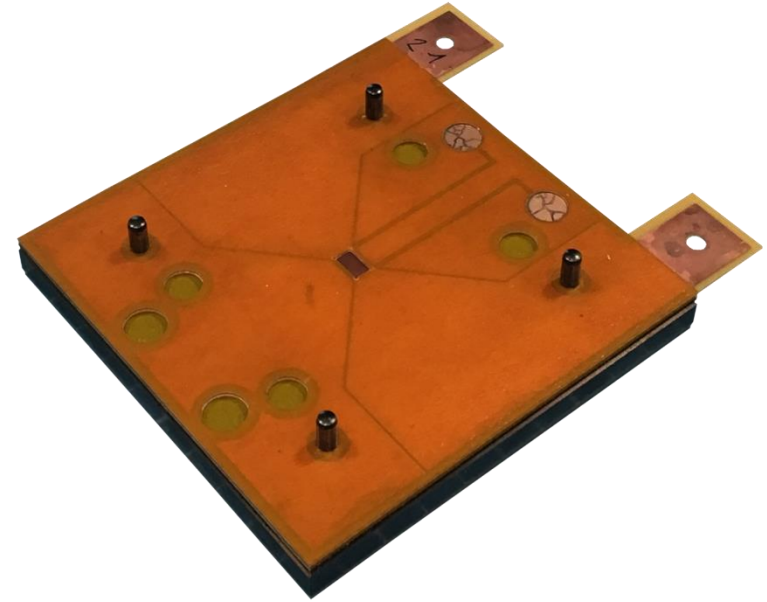


Figure 9: Stacking of the different elements of the prototype

## Test vehicles assembly

Preparation of the support  
Macro-nano structured PCB substrate  
Prepreg Arlon 35N 106

### ➤ Core Arlon 35N

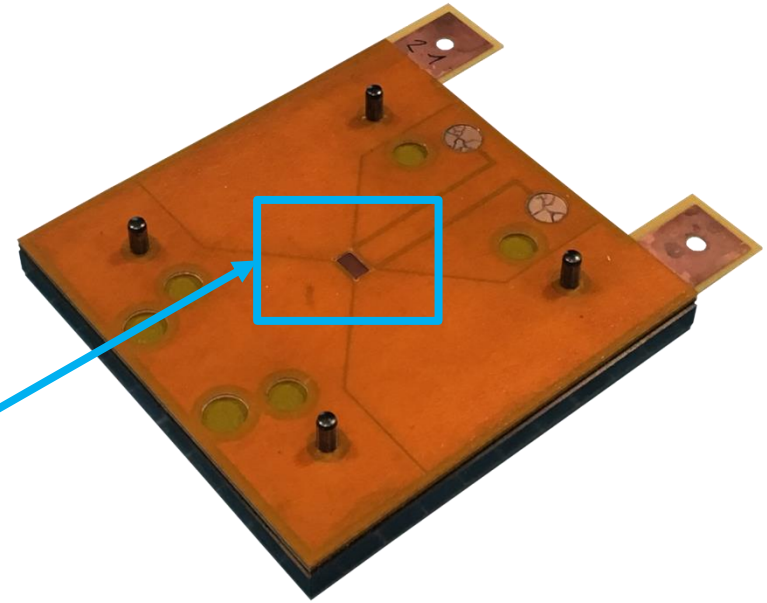
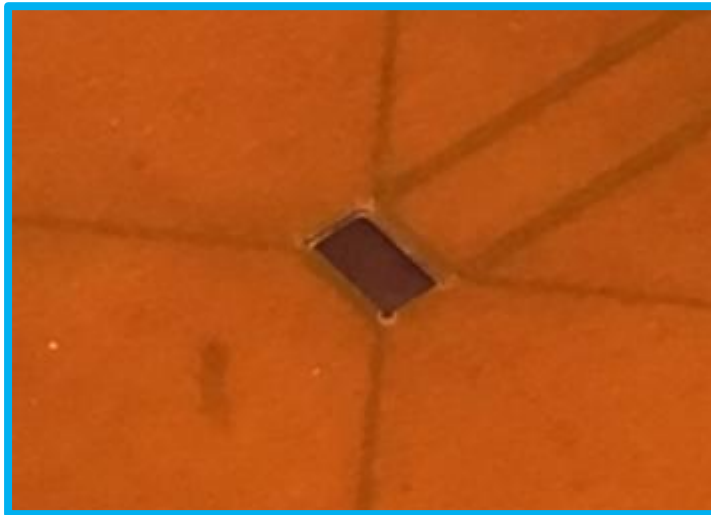


Figure 9: Stacking of the different elements of the prototype

## Test vehicles assembly

Preparation of the support  
Macro-nano structured PCB substrate  
Prepreg Arlon 35N 106  
Core Arlon 35N

### ➤ Bare die

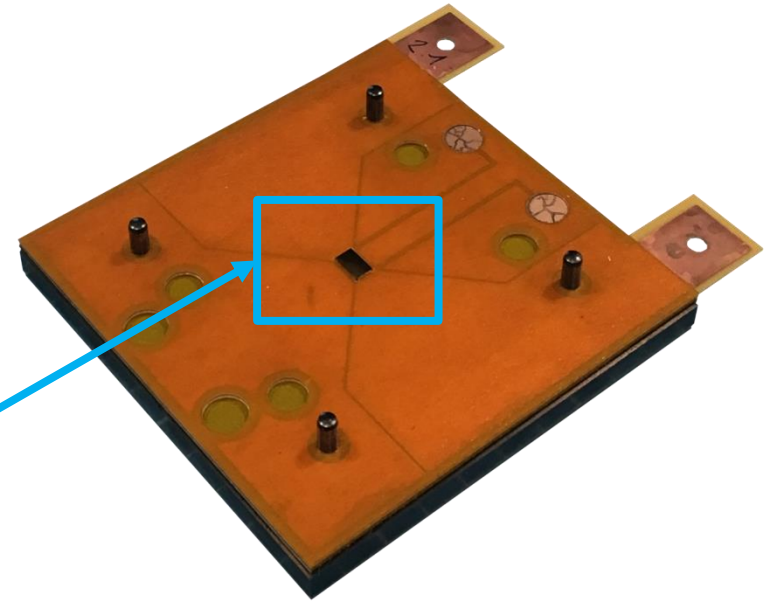
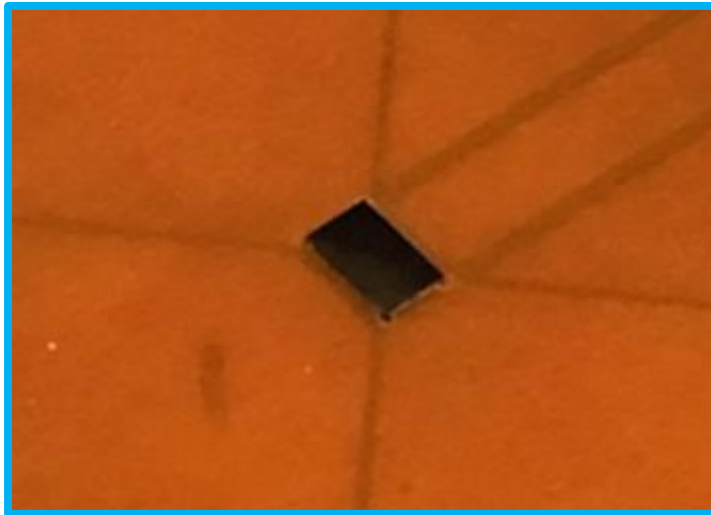


Figure 9: Stacking of the different elements of the prototype

## Test vehicles assembly

Preparation of the support  
Macro-nano structured PCB substrate  
Prepreg Arlon 35N 106  
Core Arlon 35N  
Bare die

### ➤ Prepreg Arlon 35N 106

a. Laser cut-out.

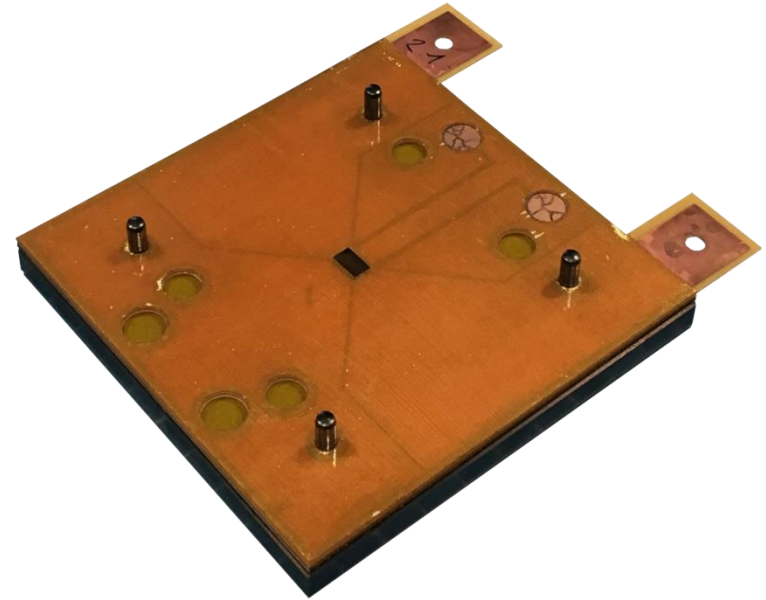


Figure 9: Stacking of the different elements of the prototype

## Test vehicles assembly

Preparation of the support  
Macro-nano structured PCB substrate  
Prepreg Arlon 35N 106  
Core Arlon 35N  
Bare die  
Prepreg Arlon 35N 106

### ➤ Macro-nano structured PCB substrate

- Deoxidized by 10% sulfuric acid treatment;
- 12 hours annealing at 120°C.

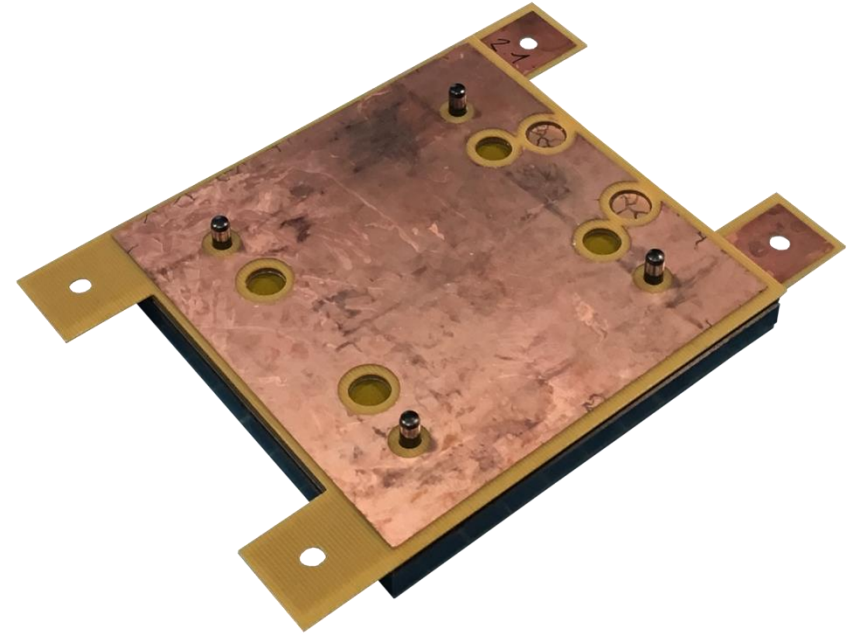


Figure 9: Stacking of the different elements of the prototype

## Test vehicles assembly

Preparation of the support

Macro-nano structured PCB substrate

Prepreg Arlon 35N 106

Core Arlon 35N

Bare die

Prepreg Arlon 35N 106

Macro-nano structured PCB substrate

### ➤ Closing of the support

- Implementation of the release films and the press pad and therefore the top plate;
- 1 hour under vacuum;
- Protective layers on both sides.

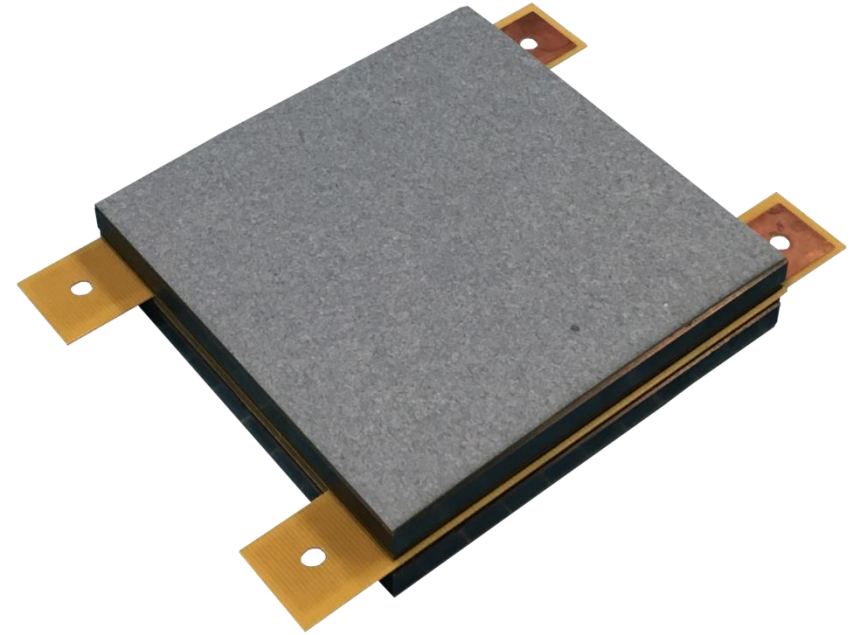


Figure 9: Stacking of the different elements of the prototype

## Test vehicles assembly

Preparation of the support  
Macro-nano structured PCB substrate  
Prepreg Arlon 35N 106  
Core Arlon 35N  
Bare die  
Prepreg Arlon 35N 106  
Macro-nano structured PCB substrate  
Closing of the support

### ➤ Pressing of the prototype

- Pressing with Arlon 35N recommended profile;
- Removing of the assembly from the support.

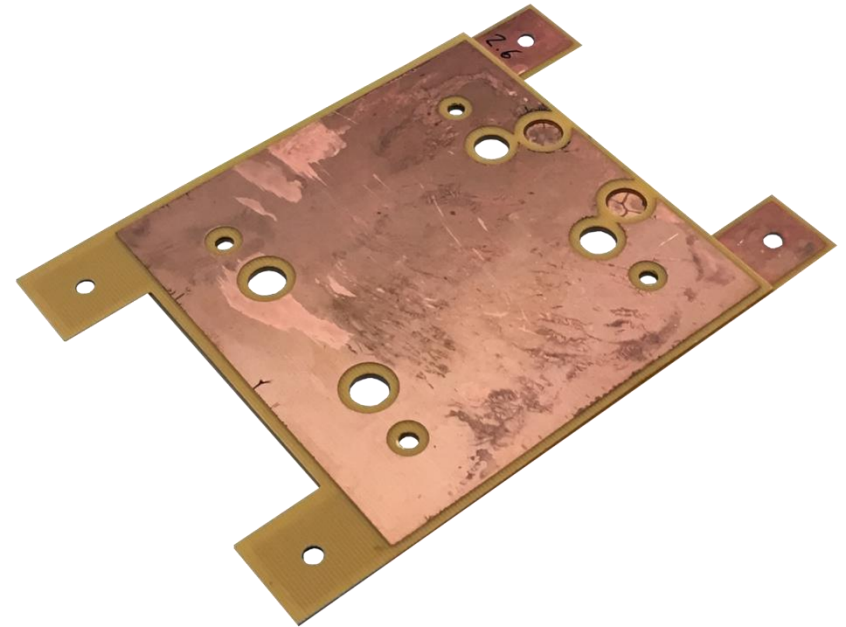


**Figure 9: Stacking of the different elements of the prototype**

## Test vehicles assembly

Preparation of the support

Macro-nano structured PCB substrate

Prepreg Arlon 35N 106

Core Arlon 35N

Bare die

Prepreg Arlon 35N 106

Macro-nano structured PCB substrate

Closing of the support

Pressing of the prototype

### ➤ Caption

- Measuring pads of (A) bottom and (B) top substrate;
- Power connectors of (C) top and (D) bottom substrate.

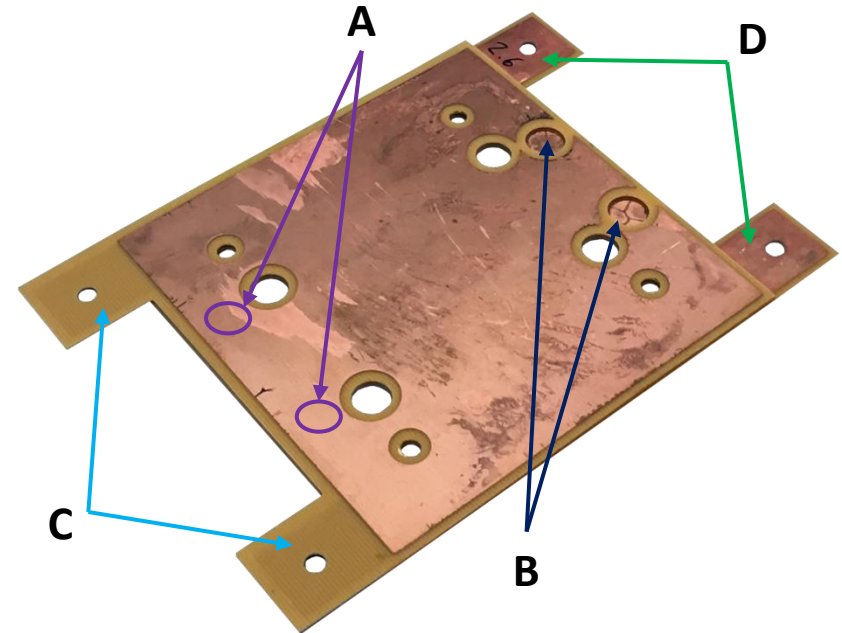


Figure 9: Stacking of the different elements of the prototype

Introduction

Context

Manufacturing process

Experimental results

Conclusion

## Electrical characterization

### Interconnection assembly

- Bare PCB substrate (a)
- Assembled by thermo-compression of a prepreg (b)
- To macro-nano structured ( $\approx 100 \mu\text{m}$ ) PCB substrate (c)

### Characterization

Two assemblies with different prepreg (interlayer)

- A  $120 \mu\text{m}$  layer of prepreg (study case A)
- A  $80 \mu\text{m}$  layer of prepreg (study case B)

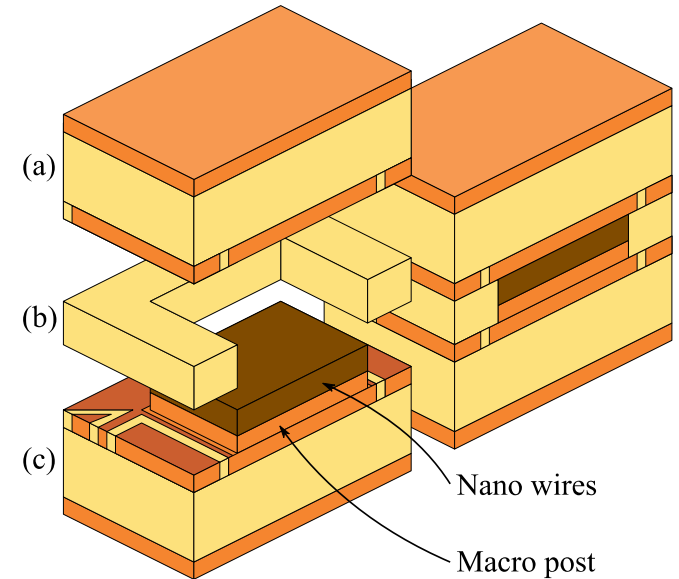


**Figure 10: Schematic of the characterization assembly**

## Electrical characterization

### Kelvin measurement

- Constricted area electrical resistance ( $R_{TOP}$  and  $R_{BOT}$ )
- Interconnection one ( $R_{INT}$ )
- Voltage measure by measuring pads ( $K_{TX}$  and  $K_{BX}$  shunted)
- Current source by power connectors ( $P_{TX}$  and  $P_{BX}$  shunted)

### Interconnection values

Proto. = 2 x Interco. + Die

Sample (Interlayer)	Int. A (120 $\mu$ m)	Int. B (80 $\mu$ m)	Die	Proto. (490 $\mu$ m)
Electrical Resistance	10 m $\Omega$	30 $\mu\Omega$	100 $\mu\Omega$	160 $\mu\Omega$

NB: Table's +/- 5% rounded measurements taken at room temperature

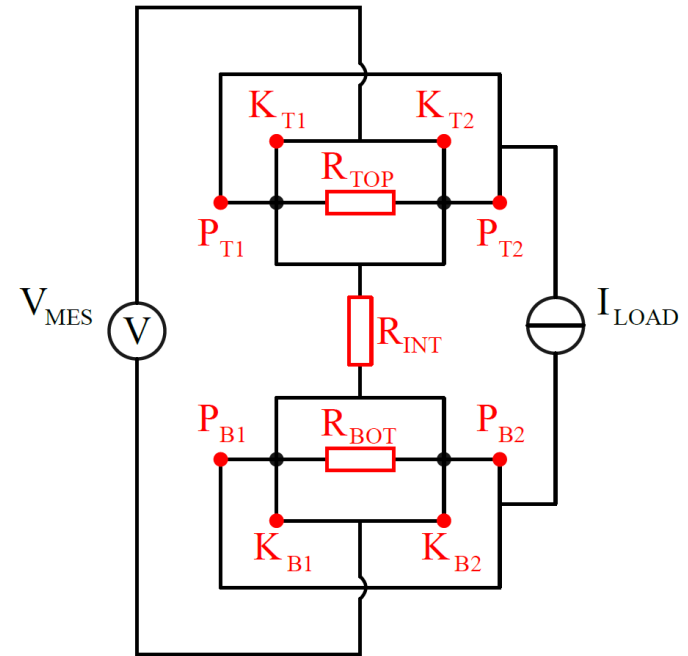


Figure 11: Electrical circuit wiring for interconnection kelvin measurement

## Electro-thermal characterization

### Evaluating of thermal resistance ( $R_{th}$ ) by

1. Controlling power flux on one side (P)
2. Measuring applied heat on the other ( $\Delta T$ )

### Constricted tracks

- ✓ Generating the heat by current applying
- ✓ Measuring of the temperature

### Furthermore

- Simulation of the power dissipated by the interconnection environment
- Assembly modification to maintain the temperature (accurate  $\Delta T$ )

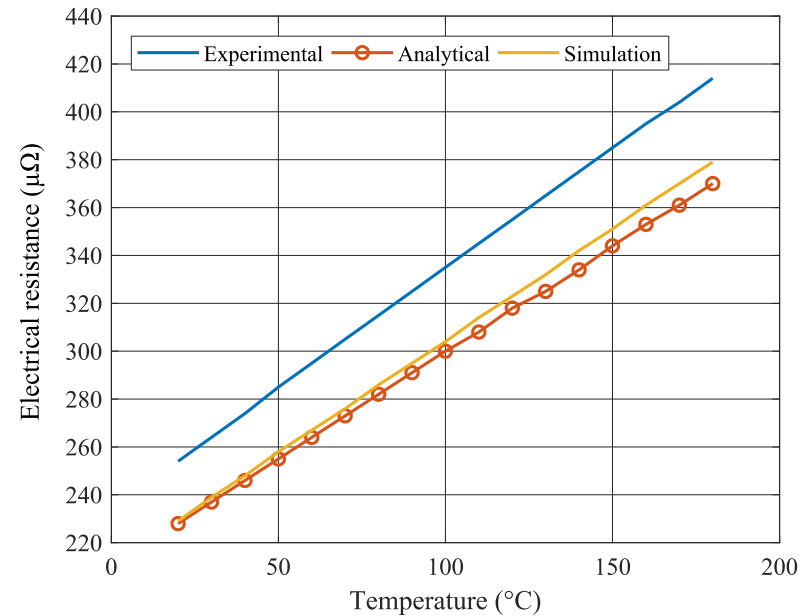


**Figure 12: Experimental, analytical and simulated curves of the constriction track**

Introduction

Context

Manufacturing process

Experimental results

Conclusion

## Evolution of the power modules

- Power semiconductor devices integration is sought

## Proposed approach

- PCB-embedding technology
- Macro-nano structured interconnections

## Best advantages

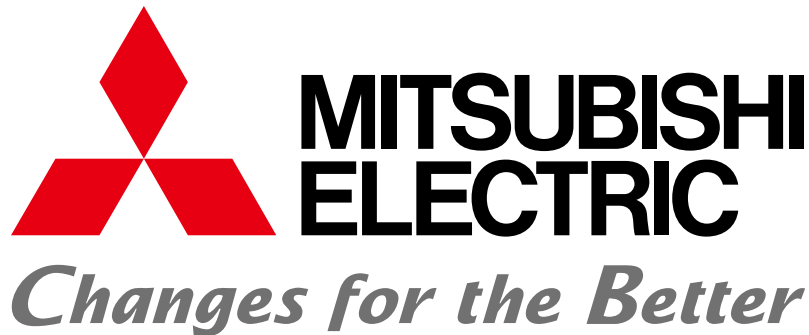
- Flex interconnection
- Double side heat dissipation
- Low stray inductances
- Manufacturing process (common electronics product line and mass production)

## Experimental results

- Parallel electroplating and electro-etching validated
- Low interconnection resistance approximatively  $115 \mu\Omega.\text{cm}^{-2}$
- Thermal resistance's measure in progress

# Thank you for your attention.

b.djuric@fr.mercede.mee.com



This work is carried out as part of a partnership between Mitsubishi Electric R&D Centre Europe, Rennes and the Laplace laboratory of the University of Toulouse.



MiNaPAD Forum 2019



*Shur, Michael. (2019). Wide Band Gap Semiconductor Technology: State-of-the-Art. Solid-State Electronics. 10.1016/j.sse.2019.03.020.*

*N. Videau et al., "5-phase interleaved buck converter with gallium nitride transistors," The 1st IEEE Workshop on Wide Bandgap Power Devices and Applications, Columbus, OH, 2013, pp. 190-193.*

*M. Meisser, M. Schmenger and T. Blank, "Parasitics in Power Electronic Modules: How parasitic inductance influences switching and how it can be minimized," Proceedings of PCIM Europe 2015; International Exhibition and Conference for Power Electronics, Intelligent Motion, Renewable Energy and Energy Management, Nuremberg, Germany, 2015, pp. 1-8.*

*B. Vidal, Paul-Etienne and Medjahed, Hassen and Nogarède, "Thermo-mechanical stress of bonded wires used in high power modules with Alternating and Direct Current modes," vol. 52, pp. 1099–1104, 2012.*

*R. Gilardoni, "Ribbon Bonding for High Frequency Applications Advantages of Ribbon and the Impact on the Microwave Market."*

*J. G. Bai, J. N. Calata, and G.-Q. L. G.-Q. Lu, “Comparative thermal and thermomechanical analyses of solder-bump and direct-solder bonded power device packages having double-sided cooling capability,” Ninet. Annu. IEEE Appl. Power Electron. Conf. Expo. 2004. APEC '04., vol. 2, no. C, pp. 1240–1246, 2004.*

*K. Siddabattula, Z. Chen, and D. Boroyevich, “Evaluation of Metal Post Interconnected Parallel Plate Structure for Power Electronic Building Blocks,” 2000.*

*W. San, D. Risaletto, F. Richardeau, G. Blondel, M. Chemin, and P. Baudesson, “Microelectronics Reliability Preliminary failure-mode characterization of emerging direct-lead-bonding power module . Comparison with standard wire-bonding interconnection,” vol. 55, pp. 1956–1960, 2015.*

*J. Xu, “Technology for Planar Power Semiconductor Devices Package with Improved Voltage Rating,” 2008.*

*Y. Zhao et al., "Silver sintering die attach process for IGBT power module production," 2017 IEEE Applied Power Electronics Conference and Exposition (APEC), Tampa, FL, 2017, pp. 3091-3094.*

*L. Ménager, B. Allard, and V. Bley, "Conditionnement des modules de puissance."*

*W. D. Macdonald and T. W. Eagar, "TRANSIENT LIQUID PHASE BONDING PROCESSES Abstract."*

*E. Vagnon, J. Crebier, Y. Avenas, and P.-O. Jeannin, "Etudes de faisabilité d'un module de puissance 3D de type press-pack pour des applications de faible et moyenne puissances," Hal, 2008.*

*Y. Zhang, T. Hammam, I. Belov, T. Sjogren, M. Bakowski, and H.-P. Nee, "Thermomechanical Analysis and Characterization of a Press-Pack Structure for SiC Power Module Packaging Applications," IEEE Trans. Components, Packag. Manuf. Technol., vol. 7, no. 7, pp. 1089–1100, 2017.*

*M. Bassem, “Assemblages innovants en électronique de puissance utilisant la technique de Spark Plasma Sintering,” 2013.*

*R. A. Beaupre, A. V. Gowda, L. D. Stevanovic, and S. A. Solovitz, “Double side cooled power module with power overlay,” 2016.*

*B. C. Charboneau et al., “Double-sided liquid cooling for power semiconductor devices using embedded power packaging,” in Fortieth IAS Annual Meeting. Conference Record of the 2005 Industry Applications Conference, 2005.*

*Y. Tanaka, K. Ota, H. Miyano, Y. Shigenaga, T. Iizuka, and K. Tatsumi, “High Temperature Resistant Packaging for SiC Power Devices Using Interconnections Formed by Ni,” no. 1, pp. 1371–1376, 2015.*

*G. Regnat and H. Id, “Onduleu a forte intégration utilisant des semi-conducteur a grand gap.”*

*K. Mohan and N. Shahane, “Nanoporous Copper for Reliable , High-Temperature and High-Power Die-Attach Interconnections,” pp. 3083–3090, 2017.*

*Y. Pascal, D. Labrousse, M. Petit, S. Lefebvre, F. Costa, and C. National, "PCB - Embedding of Power Dies Using Pressed Metal Foam," no. June, pp. 5–7, 2018.*

*B. Mouawad et al., "3-Dimensional , Solder-Free Interconnect Technology for High-Performance Power Modules," vol. 9, pp. 1–6.*

*"Carbon Nanotubes Properties and Applications," Cheap Tubes Inc., 2018.*

*V. H. Nguyen et al., "Fabrication of bottom die substrate solderless interconnection based on nano copper wires Keywords Fabrication technique AAO template," pp. 1–9.*